Modification of the photoconducting properties of ZnO thin films via low-temperature annealing and air exposure

G. Bridoux,[1, a] G. D. Ruano,[2] J. M. Ferreyra,[1] and M. Villafuerte[1]
[1] *Laboratorio de Física del Sólido, INFINOA (CONICET-UNT), Facultad de Ciencias Exactas y Tecnología, Universidad Nacional de Tucumán, 4000 San Miguel de Tucumán, Argentina*
[2] *Instituto de Física del Litoral (IFIS), S3000GLN Santa Fe, Argentina*

(Dated: 6 October 2020)

A simple thermal annealing at 150°C followed by exposure to air ambient conditions in epitaxial ZnO thin films produces a photoconductivity enhancement and a reduction of the energy gap. The first effect is related to a release of carriers from bulk traps while the second is caused by a gradual adsorption of species on the film surface which increases the band bending, as X-ray photoemission spectroscopy (XPS) shows. An observed drift of the photoconductivity and the energy gap over the days is connected to this adsorption kinetics. These findings have a potential application in ZnO based optoelectronic devices.

PACS numbers: 72.40.+w, 72.20.Jv

ZnO is a low-cost wide band gap semiconductor and a promising alternative to GaN based optoelectronic devices due to their similar crystal and electronic properties[1,2]. For its large-scale implementation, it is necessary an improved knowledge and control of: i) Intrinsic point defects[3,4] (e.g. donor oxygen vacancies, V_O, which provides a robust n-type character[5,6]) and ii) the adsorption of species on its polar surfaces (e.g. water or hydrogen resulting from the dissociation of the former[7–11]). This latter process can provide charge to the surface modifying in this way the band bending in the proximities of it[12]. In this regard, photoconductivity provides information about intrinsic point defects through their role as carrier traps or recombination centers[13–16]. Additionally, photoconductance spectroscopy is a suitable tool to extract the effective energy gap E_G (defined as the band to band transition of the conducting photoelectrons), which can be modified by band bending in nano-structures, according to the Franz-Keldysh effect[17–19]. By means of XPS, previous reports have studied the modification of the band bending properties of ZnO crystals[9,20] or thin films[21] using thermal annealing above ~ 500°C. At such a high temperature, the defect structure can be modified and it is difficult to discern its contribution to the band bending from that of the adsorbed species. Besides, surface reconstruction can take place[7–11] at such a high temperature. In the present work, we have been able to modify the photoconductance spectra of ZnO thin films after a low-temperature annealing at ~ 150°C and its subsequent exposure to ambient conditions. This study was complemented by XPS measurements and the contribution of defects and adsorbed species to the observed effects was analyzed.

ZnO films were grown on (0001) sapphire substrates (MSE Supplies) by pulsed laser deposition (PLD) using a Neocera PLD system (Model: Pioneer 120 Advanced) starting from a fabricated ZnO target (99.99 %). During the growing process, the temperature was fixed at 550°C and the oxygen pressure at 0.05 mTorr (Linde, Oxygen purity level of 99.999 %). A Nd:YAG laser (Continuum, Model: SL III-10) was operated at a wavelength of 266 nm with an energy density of $2.1\,\mathrm{J\,cm^{-2}}$, a repetition rate of 10 Hz and a deposition rate of $0.018\,\mathrm{nm\,s^{-1}}$. X-ray diffraction patterns were performed using CuKα radiation ($\lambda = 0.15406$ nm) of a Panalytical-Empyrean system. The results show that the films grew epitaxially in the [0001] direction[19]. From the Kiessig fringes observed in the low-angle $\theta - 2\theta$ scan[19], a thickness value of $t \simeq 54$ nm was determined. The post-growth thermal annealing performed in the films was at 150°C during 1 hour at a base pressure of $\sim 1 \times 10^{-6}$ Torr (labeled as TA). After the TA, the films were exposed to ambient conditions in a room with a controlled temperature (21-23°C) and relative humidity (35-40 %). Then, photoconductance and XPS spectroscopy were used to monitor their behavior over the days[21]. Photoconductance measurements were performed in a Janis (Model: CCS 350S) cryostat equipped with an optical window, a 1000 W Xe lamp plus an Oriel (Model: Cornerstone 130) monochromator with an approximate flux density of $\sim 10\,\mu W\,\mathrm{cm^{-2}}$. XPS measurements were performed using a Specs spectrometer equipped with a Phoibos 150 electrostatic hemispherical analyzer (150 mm). The detector axis was located in a position normal to the film surface. A monochromatic X-ray beam of 1486 eV energy (AlKα) was used as excitation source. The O 1s spectra were acquired in the mode of constant analyzer energy with a pass energy of 10 eV. For electrons of roughly 950 eV of kinetic energy (from O 1s) the inelastic mean free path is approximately 1.6 nm (i.e. photoelectrons from fourth atomic layer of ZnO are only detected with a probability of 0.25). The results presented in this work are representative of all the studied films. The conductivity in dark of the films was $\sigma_{dark} = 156.6\,\Omega^{-1}\mathrm{m}^{-1}$ while the carrier concentration obtained from Hall effect measurements[14] was $\bar{n} = 2.6 \times 10^{17}\,\mathrm{cm^{-3}}$ and they did

[a] Electronic mail: gbridoux@herrera.unt.edu.ar

not vary after the TA's.

Fig. 1a shows the photoconductance spectrum of the film in the as-grown conditions and how the spectrum evolves over the days after the first TA (labeled as TA-1) and the subsequent exposure to air. Several days after air exposure, a second TA (labeled as TA-2) was performed on the film and its spectrum was also monitored over the days. As it can be observed, there is an initial increment of the photoconductivity (defined as $PC = (\sigma - \sigma_{dark})/\sigma_{dark}$) after TA-2, see Fig. 1a. From this initial value of PC, it should also be noticed that PC slightly decreases over the days, see Fig. 1a. This effect is more evident when the PC values extracted from these spectra are plotted as a function of the elapsed time, see Fig. 1b. As it can be noticed, this drift is also observed after TA-1.

The initial increment of the PC value after each TA (which is more evident after TA-2) can be related to a progressive release of carriers from overall neutral defects after each annealing. In this way, these defects will become charged and hence efficient as carrier traps. This increment of the number of efficient traps will allow a decrease of the recombination rate[22,23] and an increment of the PC value. In the case of ZnO, point defects like zinc vacancies, V_{Zn}, or oxygen vacancies can play the role of hole and electron traps respectively[15,16,24,25]. As an example, we calculate the energy involved in the thermal ionization of an overall neutral oxygen vacancy. An overall neutral V_O can be composed of a compact singly ionized V_O^{1+} plus one weakly bound effective-mass-like electron[26]. The binding energy of this diffusive electron relative to the minimum of the conduction band (CB) is (in atomic units)[26]: $m^*/2\epsilon^2$, where $m^* = 0.22\,m_e$ and $\epsilon = 9.77$ for ZnO[27,28]. This gives a binding energy of 0.032 eV. This energy value is similar to the thermal energy provided by an annealing at 150°C ($k_BT = 0.036$ eV), confirming in this way the thermal ionization of defects after TA.

As it will be discussed later, the slight decrease of the PC value over the days can be related to a gradual neu-

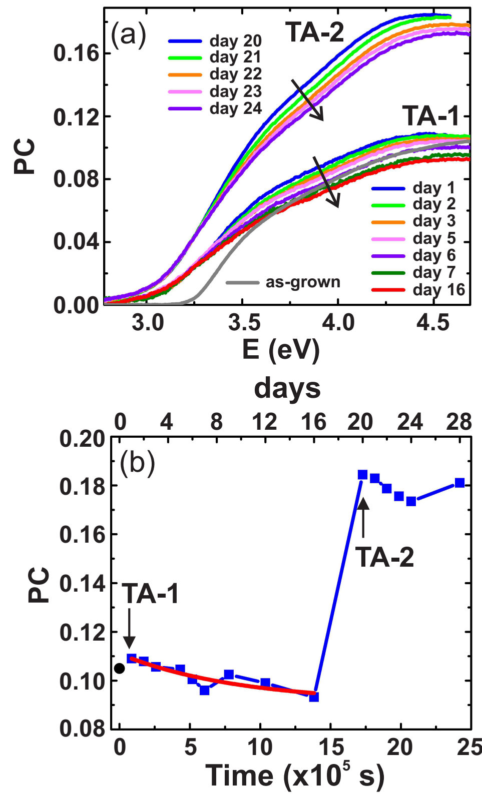

FIG. 1. (a) PC spectra after TA-1 (lower set of curves) and TA-2 (upper set of curves) monitored over the days after air exposure. The spectrum for the as-grown conditions is also shown (grey curve). The arrows indicate the increment of the days. From these spectra, the PC amplitude was extracted (b). The PC for the as-grown conditions (black dot) and an exponential fit for the PC drift over the days (red curve) are also presented.

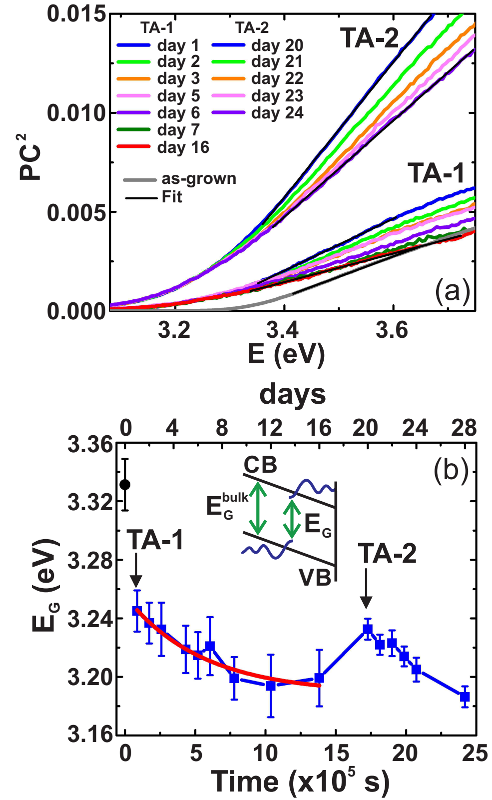

FIG. 2. (a) The spectra of Fig. 1a in the form of PC^2. Some of the linear fitting in the proximities of the onset are shown (black lines). From these fitting, E_G was extracted and its behavior over the days is also presented (b). The E_G value for the as-grown conditions (black dot) and an exponential fit for the E_G drift over the days (red curve) are also shown. The sketch illustrates the Franz-Keldysh effect and the effective energy gap, E_G.

tralization of surface defects (like V_O). This can occur if species are gradually adsorbed over the days on these surface defects inhibiting in this way their efficiency as traps. This effect will increase the recombination rate at the surface and it will slightly decrease the value of PC over the days.

Another relevant feature observed in these spectra is a red-shift of the PC onset once TA is performed, see Fig. 1a. Since in a first approximation, PC can be assumed to be proportional to the optical absorption coefficient[14,19,29], this red-shift of the onset indicates a reduction of the effective energy gap, E_G, due to the Franz-Keldysh effect, see sketch of Fig. 2. In this effect[18,19,30,31], accumulated charge on the film surface generates an electric field perpendicular to it. This electric field produces a bending of the CB and the valence band (VB) along a distance d perpendicular to the surface. This band bending allows to the electron and hole wave-functions to penetrate in the forbidden region below the bulk energy gap, E_G^{bulk}, resulting in a lower effective energy gap, E_G, see sketch of Fig. 2. The higher the band bending, V_{BB}, the lower the E_G value, as it was already shown in previous reports[19,21]. Taking into account that ZnO has a direct energy gap ($E_G^{bulk} \simeq 3.3\,\text{eV}$)[27,28] the linear relation $PC^2 \propto E - E_G$ should be fulfilled in an energy range close to the onset[21,32]. This condition is satisfied when the spectra of Fig. 1a are plotted as PC^2, see Fig. 2a. From these linear fittings, E_G can be extracted for each spectrum, and its behavior can be followed over the days after each TA, see Fig. 2b. While in the as-grown conditions the energy gap value is close to E_G^{bulk} and the bands are nearly flat, after TA and air exposure its initial value is around $E_G \simeq 3.24\,\text{eV}$ indicating an increment of the band bending. In the same way as the PC values (see Fig. 1b) the E_G values slightly decrease over the days suggesting an increment of the band bending due to a gradual accumulation of surface charge over the days. When a second TA is performed, E_G nearly recovers its initial value indicating that TA-2 partially removes the accumulated charge during the previous stage, see Fig. 2b.

In order to gather more information about the adsorbed species on the ZnO surface we have also recorded the O 1s core level XPS spectra over the days after TA and air exposure, see Fig. 3. These spectra were fitted using three pseudo-Voigt functions after subtracting a linear baseline, keeping the full width at half maximum and the energetic separation of the three peaks constrained. These pseudo-Voigt functions are calculated according to the Doniach-Sjunic algorithm with the following parameters: Gaussian width=1 eV, Lorentzian width=0.2 eV, asymmetry=0 and the relative energy of the smaller contributions respect to the main peak at 1.4 eV and 2.6 eV. The main component is associated to bulk oxygen emission. In the case of an O-polar ZnO surface, previous reports[8–10,33] suggest that the second component (shifted to higher binding energy by $\sim$ 1.4 eV) comes from a surface oxygen that forms a hydroxyl (OH) group with an hydrogen atom (originated from water dissociation), while the third component (around $\sim$ 533.5 eV) is related to molecular water adsorbed on the ZnO surface or

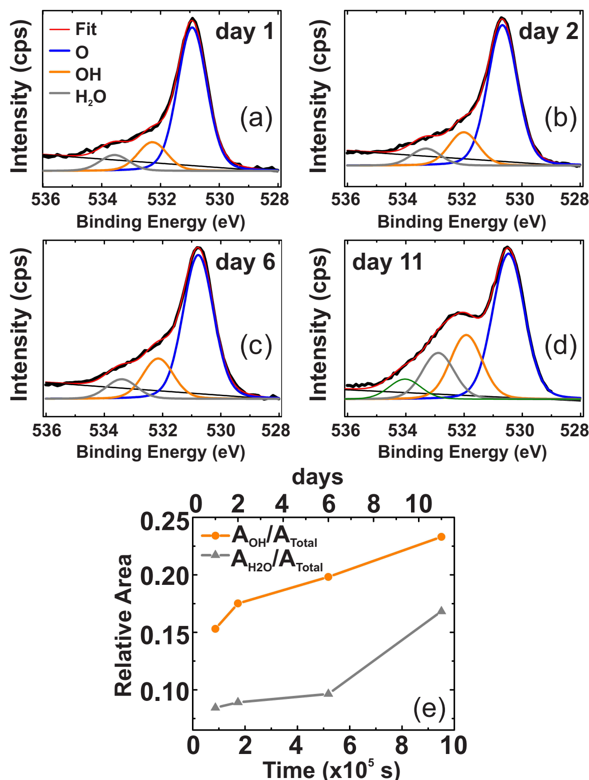

FIG. 3. (a)-(d) Evolution over the days of the O 1s core level XPS spectrum after TA-1 and subsequent air exposure. The spectrum was fitted using three components after a linear background subtraction. A fourth component was required at day 11. (e) Relative peak area of each component over the days after TA-1 and air exposure.

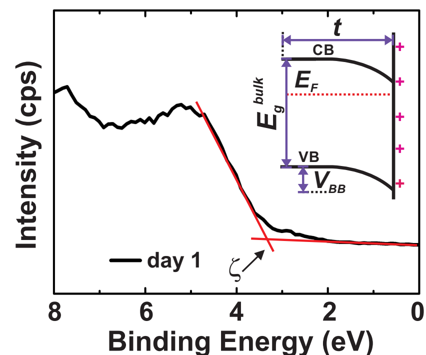

FIG. 4. Valence band XPS spectrum recorded a day after TA-1. From the intersection of the two linear fits (red lines) ζ can be obtained. The sketch represents the energy band diagram after TA and air exposure.

on top of these (OH) groups[34,35]. Fig. 3e shows that the area of the second (A_{OH}) and third component (A_{H_2O}) relative to the total area (A_{Total}) gradually increase over the days indicating that the PC and E_G drift (Fig. 1b and Fig. 2b respectively) are related to a hydrogenation of the surface. Indeed, the hydrogenation increment (defined as $(A_{OH}+A_{H_2O})/A_{Total}$) from day 1 to 11 is around $\sim 70\,\%$.

In particular, the slow decrease of the PC value over the days observed in Fig. 1b can be related to a gradual adsorption of water or (OH) on surface oxygen vacancies[36]. As it was already mentioned, this adsorption process can inhibit or neutralize the role of the surface defects (in this case surface V_O) as efficient carrier traps leading in this way to a slight decrease of the PC value over the days. Anion hydrogen can also be adsorbed in these surface V_O forming a complex[37] V_O^{2+}-2H$^-$ that is no longer efficient as electron trap.

On the other hand, it would be of interest to confirm the presence of a band bending after the thermal annealing and to determine its value and sign, that is, if there is an upward or a downward band bending after the TA[21]. In order to do that, we have measured the valence band XPS spectrum of the film a day after TA and air exposure, see Fig. 4. If the onset value, ζ, is extracted from this low-energy spectrum, the band bending value can be obtained as follows[9]: $V_{BB} = E_G^{bulk} - \zeta - \xi$, where ξ is the energy difference between the Fermi energy level and the minimum of the CB. ξ can be expressed as follows: $\xi = (k_B T/q)\ln(N_c/\bar{n})$, where N_c is the CB effective density of states ($N_c = 2.94\times 10^{18}\,\mathrm{cm}^{-3}$ for ZnO[9]). Since $\xi \simeq 0.20\,\mathrm{eV}$ and $\zeta \simeq 3.17\,\mathrm{eV}$, we obtain a value of $V_{BB} \simeq -0.04\,\mathrm{eV}$. This negative value of V_{BB} implies that a downward band bending is established after TA and the exposure to air, see sketch of Fig. 4. In general[12], a downward band bending is produced by the accumulation of positive charge on the surface. In this case, this charge is provided by hydrogen-like species that gradually adsorb in the film surface[9,38], as core level XPS spectra show, see Fig. 3. These results also confirm that the band bending is the responsible of the reduction of E_G, see Fig. 2b.

In order to gain more insight on the slow adsorption kinetics, we have assumed that the relaxation time involved in the fraction of occupied surface sites[39], $\theta(t) \simeq 1 - e^{-t/\tau}$, is connected to the one obtained by fitting the PC and E_G drift with an exponential decaying function, see Fig. 1b and Fig. 2b. Taking into account that τ is related to the activation energy for adsorption via[40] $E_a = k_B T\,\ln(\nu\,\tau)$, and considering that[21] $\nu \simeq 4.8\times 10^{10}\,\mathrm{s}^{-1}$ we obtain $E_a \simeq 0.96\,\mathrm{eV}$ for the extracted relaxation times $\tau = 5.4\times 10^5\,\mathrm{s}$ and $8.4\times 10^5\,\mathrm{s}$.

Finally, it is worth to make a general comparison between this work and previous studies in ZnO[9,20,21] where high-temperature annealing (above $\sim 500°$C) were performed. One of the main differences resides in the fact that at such a high temperatures oxygen diffusion occurs and it can modify the number of oxygen vacancies in the proximities of the surface. As a consequence, the density of traps and the carrier concentration can vary significantly affecting in this way the band bending and the value of PC. In one of these studies[21], the PC value is not enhanced after a cycle of several annealing in contrast to our findings. Besides, at such a high-temperature annealing, atomic surface reconstruction or a modification of the surface morphology can take place[8,10,41,42] and they can affect the adsorption kinetics and the band bending properties.

In conclusion, this work shows how a simple low-temperature annealing at 150°C can modify the photoconducting properties of ZnO thin films. Successive thermal annealing enhance the PC which can be associated to a release of electrons or holes from bulk traps. The first thermal annealing also generates a reduction of E_G from $\simeq 3.3\,\mathrm{eV}$ to $\simeq 3.24\,\mathrm{eV}$ due to an increment of the band bending caused by an enhanced role of adsorbed hydrogen as positive surface charge, as XPS confirms. A gradual decrease of PC and E_G over the days after this thermal annealing was also observed and it is related to a slow adsorption rate of hydrogen-like species, as XPS shows. These species can inhibit the efficiency of surface traps leading to this slight decrease of PC. Besides, a second thermal annealing nearly recovers the initial E_G value obtained after the first thermal annealing. As a perspective, it would be interesting for applications to investigate the behavior of the PC in a multi-annealing cycle using different atmospheric conditions. This modification of the photoconducting properties of ZnO thin films in such an easy way can be of potential interest for technological applications.

ACKNOWLEDGMENTS

This work was supported by PIP- No. 585, SCAIT-No. E653CX, PICT- No. 2016-3356 , SNMAG and SINALA facilities. We acknowledge to G. Zampieri.

[1] Ü. Özgür, D. Hofstetter and H. Morkoç, Proc. IEEE **98**, 1255 (2010).
[2] C. W. Litton, T. C. Collins, D. C. Reynolds, *Zinc Oxide Materials for Electronic and Optoelectronic Device Applications* (Wiley, Chichester, 2011).
[3] A. Janotti and C. G. Van de Walle, Phys. Rev. B **76**, 165202 (2007).
[4] A. Janotti and C. G. Van de Walle, Appl. Phys. Lett. **87**, 122102 (2005).
[5] L. E. Halliburton, N. C. Giles, N. Y. Garces, M. Luo, C. Xu, L. Bai and L. A. Boatner, Appl. Phys. Lett. **87**, 172108 (2005).
[6] L. Liu, Z. Mei, A. Tang, A. Azarov, A. Kuznetsov, Q. -K. Xue and X. Du, Phys. Rev. B **93**, 235305 (2016).
[7] B. Meyer and D. Marx, Phys. Rev. B **67**, 035403 (2003).
[8] J. V. Lauritsen, S. Porsgaard, M. K. Rasmussen, M. C. R. Jensen, R. Bechstein, K. Meinander, B. S. Clausen, S. Helveg, R. Wahl, G. Kresse and F. Besenbacher, ACS Nano **5**, 5987 (2011).
[9] R. Heinhold, G. T. Williams, S. P. Cooil, D. A. Evans and M. W. Allen, Phys. Rev. B **88**, 235315 (2013).
[10] S. Erker, P. Rinke, N. Moll and O. T. Hofmann, New J. Phys. **19**, 083012 (2017).

[11]M. Iachella, J. Cure, M. Djafari Rouhani, Y. Chabal, C. Rossi and Alain Estève J. Phys. Chem. C **122**, 21861 (2018).
[12]Z. Zhang and J. T. Yates Jr., Chem. Rev., **112**, 5520 (2012).
[13]R. H. Bube, *Photoconductivity of Solids*, (John Wiley and Sons, Inc., 1960).
[14]G. Bridoux, M. Villafuerte, J. M. Ferreyra, N. Bachi, C. A. Figueroa and S. P. Heluani, Phys. Rev. B **92**, 155202 (2015).
[15]M. Villafuerte, D. J. Zamora, G. Bridoux, J. M. Ferreyra, M. Meyer and S. P. Heluani, J. Appl. Phys. **121**, 064501 (2017).
[16]J. M. Ferreyra, G. Bridoux, M. Villafuerte, B. Straube, J. Zamora, C. A. Figueroa and S. P. Heluani, Sol. State Commun. **257** 42 (2017).
[17]C. Wetzel, T. Takeuchi, H. Amano and I. Akasaki, J. Appl. Phys. **85**, 3786 (1999).
[18]A. Cavallini, L. Polenta, M. Rossi, T. Stoica, R. Calarco, R. J. Meijers, T. Richter and H. Lüth, Nano Letters **7**, 2166 (2007).
[19]G. Bridoux, M. Villafuerte, J. M. Ferreyra, J. Guimpel, G. Nieva, C. A. Figueroa, B. Straube and S. P. Heluani, Appl. Phys. Lett. **112**, 092101 (2018).
[20]R. Heinhold, S. P. Cooil, D. A. Evans and M. W. Allen, J. Phys. Chem. C **118**, 24575 (2014).
[21]G. Bridoux, G. D. Ruano, J. M. Ferreyra and M. Villafuerte, J. Appl. Phys. **127** 245704 (2020).
[22]C. Soci, A. Zhang, B. Xiang, S. Dayeh, D. Aplin, J. Park, X. Bao, Y. Lo, and D. Wang, Nano Letters **7**, 1003 (2007).
[23]S. F. Chichibu, A. Uedono, K. Kojima, K. Koike, M. Yano, S. Gonda and S. Ishibashi, J. Appl. Phys. **127**, 215704 (2020).
[24]T. J. Penfold, J. Szlachetko, F. G. Santomauro, A. Britz, W. Gawelda, G. Doumy, A. M. March, S. H. Southworth, J. Rittmann, R. Abela, M. Chergui and C. J. Milne, Nat. Comm. **9**, 478 (2018).
[25]C. Figueroa, B. Straube, M. Villafuerte, G. Bridoux, J. Ferreyra, N. C. Vega and S. P. Heluani, J. Appl. Phys. **127**, 045703 (2020).
[26]J. Buckeridge, C. R. A. Catlow, M. R. Farrow, A. J. Logsdail, D. O. Scanlon, T. W. Keal, P. Sherwood, S. M. Woodley, A. A. Sokol and A. Walsh, Phys. Rev. Mat. **2**, 054604 (2018).
[27]H. Morkoç and Ü. Özgür, *Zinc Oxide* (Wiley-VHC, Weinheim, 2009).
[28]M. Grundmann, *The Physics of Semiconductors*, (Springer, Heidelberg 2016).
[29]H. Zhang, L. Yan and H.-U. Habermeier, J. Phys.: Condens. Matter **25**, 035802 (2013).
[30]J. H. Davies, *The Physics of Low-Dimensional Semiconductors* (Cambridge University Press, New York, 1998).
[31]C. Lamberti, *Characterization of Semiconductor Heterostructures and Nanostructures* (Elsevier, Amsterdam, 2008).
[32]J. I. Pankove, *Optical Processes in Semiconductors* (Dover Publications, Inc., New York, 1976).
[33]A. R. McNeill,A. R. Hyndman,R. J. Reeves,A. J. Downard and M. W. Allen, ACS Appl. Mater. Interfaces **8**, 31392 (2016).
[34]J. B. L. Martins, J. Andrés, E. Longo and C. A. Taft, Int. J. Quantum Chem. **57**, 861 (1996).
[35]M. Schiek, K. Al-Shamery, M. Kunat, F. Traeger, and C. Wöll, Phys. Chem. Chem. Phys. **8**, 1505 (2006).
[36]M. Kunat, St. Gil Girol, U. Burghaus and Ch. Wöll, J. Phys. Chem. B **107**, 14350 (2003).
[37]M. -H. Du and K. Biswas, Phys. Rev. Lett. **106**, 115502 (2011).
[38]M. W. Allen, C. H. Swartz, T. H. Myers, T. D. Veal, C. F. McConville and S. M. Durbin, Phys. Rev. B **81**, 075211 (2010).
[39]N. Bundaleski, A. G. Silva, U. Schroder, A. M. C. Moutinho and O. M. N. D. Teodoro, J. Phys.: Conf. Ser. **257**, 012008 (2010).
[40]H. Lüth, *Solid surfaces, interfaces and thin films*, (Springer, Heidelberg, 2010).
[41]B. Meyer, Phys. Rev. B **69**, 045416 (2004).
[42]J. Zhang, Y. Liu, Z. Wei and J. Zhang, Appl. Surf. Sci. **265** 363 (2013).